Eye (2021) 35:1712–1720
https://doi.org/10.1038/s41433-020-01171-9

The ROYAL COLLEGE of OPHTHALMOLOGISTS

ARTICLE

Peripapillary and macular choroidal vascularity index in patients with clinically unilateral pseudoexfoliation syndrome

Mert Simsek[1] · Onur Inam[1,2] · Emine Sen[1] · Ufuk Elgin[1]

Received: 5 March 2020 / Revised: 21 August 2020 / Accepted: 24 August 2020 / Published online: 1 September 2020

Abstract

Purpose To investigate choroidal vascular changes using an image binarization tool in patients with clinically unilateral pseudoexfoliation syndrome (XFS).

Methods This cross-sectional study included 150 eyes of 100 patients. The eyes were divided into three groups: (1) 50 affected eyes of patients with clinically unilateral XFS; (2) 50 unaffected fellow eyes; and (3) 50 healthy control eyes. Enhanced depth imaging optical coherence tomography scans of the macula and peripapillary regions were acquired. Images were binarized using ImageJ software (National Institutes of Health, Bethesda, MD, USA). The choroidal vascularity index (CVI) was defined as proportion of the luminal area to the total circumscribed choroidal area.

Results Horizontal and vertical scans revealed that the macular CVI values of the affected eyes (60.08 ± 2.06 and 62.21 ± 2.10, respectively) were lower compared with control eyes (67.31 ± 2.24; $p = 0.001$ and 68.11 ± 2.36; $p < 0.001$, respectively). Conversely, no significant difference in the macular CVI was found between unaffected fellow and control eyes ($p = 0.094$ and $p = 0.120$, respectively). The mean peripapillary CVI values of the temporal (58.73 ± 3.15), superior (59.84 ± 3.09), and inferior (56.94 ± 2.47) sectors were significantly lower in affected eyes compared to control eyes (63.21 ± 3.00, 62.07 ± 3.05, and 60.78 ± 2.88, respectively; $p < 0.05$ for all). In addition, the unaffected fellow eyes had significantly lower CVI values in the temporal (61.42 ± 3.07) and inferior (57.61 ± 2.56) peripapillary sectors compared with the control eyes ($p = 0.007$ and $p = 0.005$, respectively).

Conclusions These findings suggest that XFS is associated with decreased macular and peripapillary choroidal vascularity. Furthermore, the unaffected eyes of patients with unilateral XFS may show vascularity changes in the peripapillary choroid.

Introduction

Pseudoexfoliation syndrome (XFS) is characterized by the production and progressive accumulation of whitish extracellular fibrillary material (XFM) originating from an abnormal basement membrane in ocular tissues, including the corneal endothelium, trabecular meshwork, ciliary epithelium, iris stroma, anterior lens capsule, zonules, and anterior hyaloid [1, 2]. XFM has also been demonstrated to accumulate in several extraocular tissues, including the heart, connective tissue of the lungs, skin, gallbladder, kidneys, liver, urinary bladder, meninges, and vascular endothelium [3, 4]. XFS is actually a systemic disorder associated with vascular dysfunction [5–7]. Increased homocysteine levels, a predisposition to fibrin clot formation, and impairment in vascular endothelial function all play a role in the pathogenesis of vascular dysfunction [8].

The effects of XFM on the ocular vascular structure have been investigated. It has been shown that pseudoexfoliative fibrils accumulate in the iris vessels by electron microscopy [9]. Iris fluorescein angiography revealed hypoperfusion, microneovascularization, and anastomotic vessels in the irises of these cases [10]. XFM was also identified within the walls of the posterior ciliary

Disclosure statement: The authors report no conflicts of interest and have no proprietary interest in any of the materials mentioned in this article. This article has been read and approved by all the authors. This research received no specific grant and/or equipment from any funding agency in the public, commercial, or not-for-profit sectors.

✉ Mert Simsek
mertsimsek86@gmail.com

[1] Department of Ophthalmology, University of Health Sciences, Ulucanlar Eye Education and Research Hospital, Ankara, Turkey

[2] Department of Biophysics, Faculty of Medicine, Gazi University, Ankara, Turkey

arteries and the central retinal artery, as well as in the vortex veins [11]. Reduced hemodynamic parameters of the ophthalmic artery and retrobulbar vessels have also been demonstrated by colour Doppler imaging in patients with XFS [12, 13]. In another study by Cinar et al., optical coherence tomography (OCT)-angiography demonstrated decreased choriocapillaris flow area in eyes with XFM compared to control eyes [14]. OCT-angiography provides the noninvasive assessment of the retina and the choriocapillaris blood flow. However, this approach is insufficient to evaluate the remaining choroidal vasculature. With the emergence of the latest developments in imaging methods, such as swept-source technology and enhanced depth imaging mode, more detailed information about the choroid can be obtained non-invasively.

The choroid is a layer made up of both connective and vascular tissue [15]. It plays a role in the blood supply of the prelaminar, laminar, and retrolaminar regions of the optic nerve head and the outer layers of the retina. Any choroidal vascular change can play a major role in the pathophysiology of several ocular disorders. The effects of XFS on the choroidal thickness (CT) and choroidal vessel diameter (CVD), which are parameters used to assess the choroidal vascular status, have been investigated. Choroidal thinning and decreased CVD were demonstrated in eyes with XFS [16–18]. In contrast, several other studies have reported that XFS has no effect on the CT [19–21].

The choroidal vascularity index (CVI) is a novel marker first described by Agrawal et al. [22]. The choroid can be divided into a stromal area (SA) and a luminal area (LA) using an image binarization method, which allows the vascular status to be evaluated in detail. While SA fraction (interstitial area) contains melanocytes, fibroblasts, resident immunocompetent cells, smooth muscle cells, and supporting collagenous and elastic connective tissue, LA fraction indicates all of the blood vessels [23]. The CVI is currently being extensively investigated, especially for its role in various retinal and choroid diseases [24–26]. However, the effect of pseudoexfoliation on the submacular and peripapillary CVI has not yet been investigated. Thus, the present study explored the sizes of the LA and the SA of the choroid in the affected and unaffected fellow eyes of patients with clinically unilateral XFS and compared these measurements with those of healthy control participants.

Materials and methods

Ethical approval

All participants were selected from a single tertiary eye care centre. All study procedures were carried out in accordance with the Declaration of Helsinki, and informed consent was obtained from all patients after approval from the Ethics Committee of the Ankara Training and Research Hospital (Report Number: 2019-113). All patients were Caucasian-Turkish.

Study participants and examinations

This cross-sectional and comparative study enrolled 100 eyes of 50 patients with clinically unilateral XFS who were diagnosed at the outpatient clinic of our hospital. Fifty eyes of 50 healthy sex- and age-matched participants were selected to serve as the control group. The study participants were divided into three groups: (1) an affected eye group that included the involved eyes of patients with clinically unilateral XFS, (2) an unaffected fellow eye group that included the unaffected, contralateral eyes of these patients, and (3) a healthy eye group of controls that included participants with no other ocular diseases.

The diagnoses and follow-up examinations of the patients with clinically unilateral XFS were conducted at the outpatient clinic by the same experienced physician (UE). Pseudoexfoliative material was detected clinically at the pupillary border or on the surface of the anterior lens capsule following pupillary dilation or on the trabecular meshwork with gonioscopy using slit-lamp biomicroscopy. Furthermore, pupillary ruff defects and transillumination defects reinforced the diagnosis of XFM. The control group consisted of age and sex-matched cases who had undergone a routine ocular examination at the outpatient clinic and had no other diseases or conditions. Only data from the right eyes of healthy individuals were used in the statistical analysis.

Patients that had any of the following situations were excluded from the present study: bilateral involvement of XFS, a history of ocular or orbital trauma, any previous medical or surgical ocular treatment, a history of any type of uveitis, optic disc anomalies such as coloboma, drusen, and tilted disc, a history of any type of optic neuropathies (ischemic or non-ischemic), any type of maculopathy, retinal vascular diseases such as diabetic retinopathy, hypertensive retinopathy, and vascular occlusion, autoimmune diseases, systemic vasculitis, uncontrolled hypertension with current systemic medical treatment, a spherical and/or cylindrical refractive error > 6 dioptres (D), an axial length (AL) > 24 mm and <22 mm, and smoking or alcohol use that might have caused vascular dysfunction. In addition, patients that had glaucomatous visual fields, repeated intraocular pressure (IOP) measurements of >21 mmHg, or nerve fibre layer defects by OCT analysis were excluded since these conditions may affect the vascular network.

All patients underwent a comprehensive ophthalmologic examination, including an anterior segment and a dilated posterior segment examination with a slit-lamp

biomicroscope. The demographic data of patients, their best-corrected visual acuity (BCVA) as measured by a Snellen chart (as converted LogMAR equivalent), gonioscopy using a Goldmann three-mirror lens, and IOP values measured using a noncontact pneumotonometer were performed. The spherical equivalent (SE) was determined using the following formula: spherical power +1/2 cylindrical power. The mean arterial pressure (MAP) was obtained using the following formula: diastolic blood pressure +1/3 (systolic blood pressure–diastolic blood pressure). The mean ocular perfusion pressure (MOPP) was calculated as 2/3 MAP–IOP. The central corneal thickness (CCT) and AL were measured using a Lenstar LS 900 (Hagg-Streit AG, Koeniz, Switzerland).

After a complete biomicroscopic examination was carried out, the enhanced depth imaging mode of spectral domain optical coherence tomography (EDI-SD-OCT; Spectralis, Heidelberg Engineering GmbH, Heidelberg, Germany) was used by the same experienced medical technician to conduct an exam. All OCT measurements were performed at the same time interval (between 09:00 and 11:00 a.m.) to prevent diurnal fluctuations. Furthermore, all scans were obtained after pupil dilation. Macular OCT images were acquired using horizontal and vertical scans centred on the central foveal region (Fig. 1a, b). Peripapillary OCT images were obtained using horizontal and vertical scans centred on the optic nerve head (Fig. 2a, b). Only high-quality scans (>25 Q) were evaluated. The images were viewed and measured with the Heidelberg Eye Explorer software (Heidelberg Eye Explorer version 1.8.6.0; Heidelberg Engineering). The obtained raw OCT data (submacular and peripapillary) were evaluated with an image processing program for further analysis.

Image acquisition and processing

Image processing was performed using an open-source software (http://fiji.sc/). It was binarized using the protocol described by Agrawal et al. [22]. Accordingly, the OCT scan was opened using the ImageJ 1.51 s (National Institutes of Health, Bethesda, MD, USA) platform. First, the image was binarized to view the choroid–scleral junction using the autolocal threshold tool (Niblack method, 8-bit type). A reference line was drawn parallel to the retinal pigment epithelium using the line tool. The circumscribed submacular choroidal area (TCA; 1500 µm width on four sides from the fovea) was selected as the region between the retinal pigment epithelium and choroid–scleral junction using the polygon tool. This region was added to the region of interest (ROI) manager. Next, the colour threshold tool and Red-Green-Blue color type were used to select the dark pixels expressing the LA and was saved in the ROI manager. The both areas in the ROI manager were selected and merged via an "AND" command (Fig. 1c, d). The optic nerve head images were analysed using the method described by Cetin et al. [27]. and Wang et al. [28]. In these scans, the superior, temporal, nasal, and inferior quadrants (1000 µm width on four sides from the optic disc border) of the peripapillary area were binarized separately (Fig. 2c, d). The optic disc boundary was marked at the inner margin of the scleral ring.

The CVI was calculated as the ratio of LA to TCA. The SA was indicated by light-coloured pixels and was

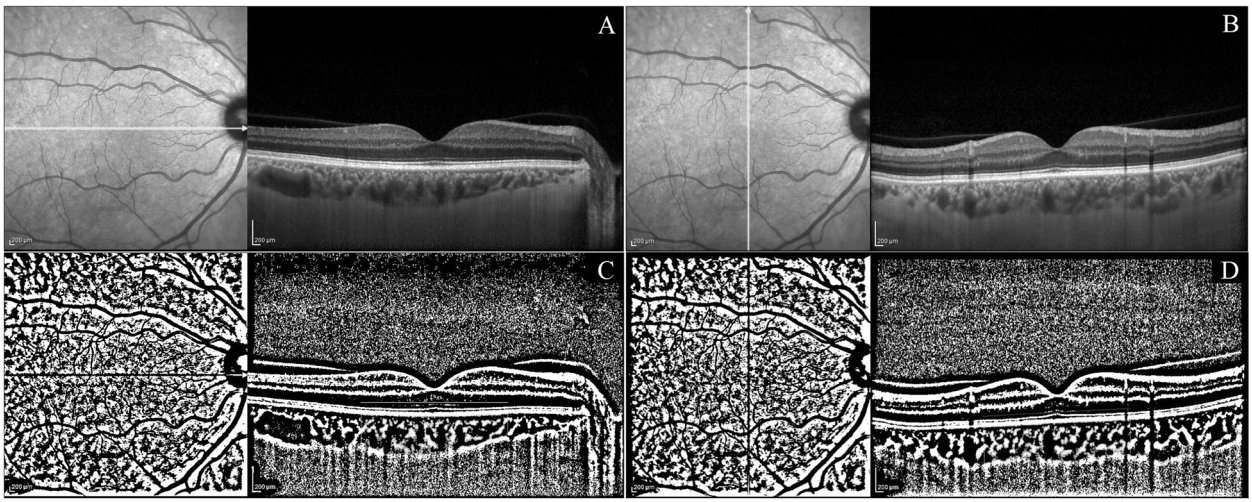

Fig. 1 Enhanced depth imaging mode of spectral domain optical coherence tomography (Spectralis, Heidelberg Engineering GmbH, Heidelberg, Germany) scans. Horizontal (**a**) and vertical (**b**) macular scans centered on the central foveal region. Illustration of submacular choroidal vascularity index measurement using ImageJ software. The scan was binarized to view the choroid-scleral junction using the autolocal threshold tool (Niblack method, 8-bit type). A 3000 µm width reference line (gray color) was drawn using the line tool and circumscribed submacular choroidal area was selected using the polygon tool. The yellow lines represented the luminal area (dark pixels) using the color threshold tool (**c**, **d**).

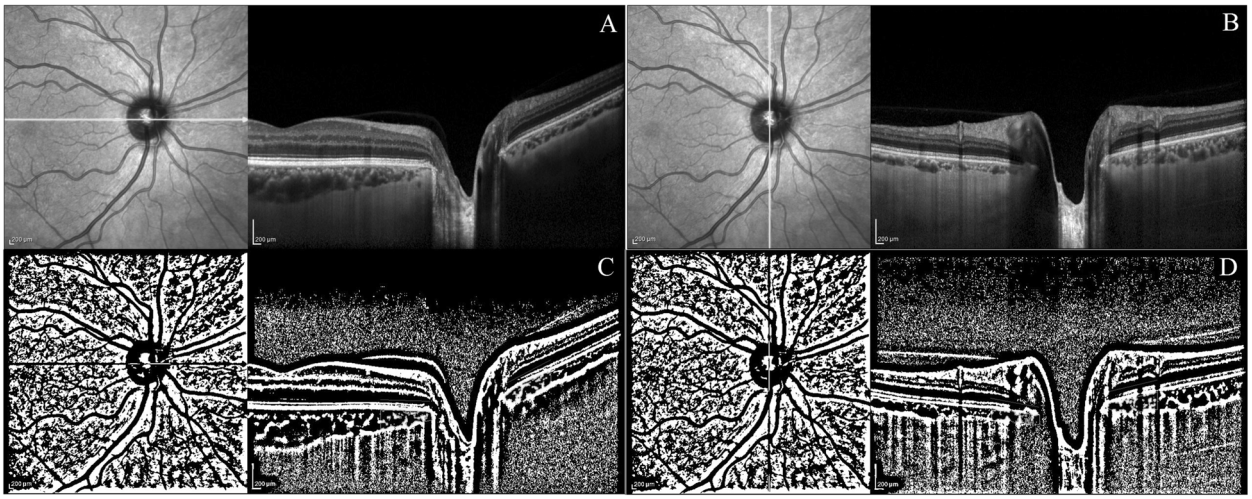

Fig. 2 Enhanced depth imaging mode of spectral domain optical coherence tomography (Spectralis, Heidelberg Engineering GmbH, Heidelberg, Germany) scans. Horizontal (temporal and nasal; **a**) and vertical (superior and inferior; **b**) peripapillary scans centered on the optic nerve head. Illustration of peripapillary choroidal vascularity index measurement using ImageJ software. The scan was binarized to view the optic disc boundary using the autolocal threshold tool (Niblack method, 8-bit type). A 1000 µm width reference line (gray color) was drawn using the line tool and circumscribed peripapillary choroidal sectors were selected using the polygon tool. The yellow lines represented the luminal area (dark pixels) of peripapillary choroidal sectors using the color threshold tool (**c**, **d**).

calculated by subtracting the LA from the TCA. The ratio of the LA to the SA (LSR) was calculated. The LSR and CVI are proportional indicators of the vascular space in the choroid. All these measurements were performed separately by two blinded researchers (MS, OI). The means of both values were included in the statistical analysis. The interobserver and intraobserver reliability of the submacular CVI (mCVI) and the peripapillary CVI (pCVI) calculations were evaluated using intraclass correlation coefficients (ICC) with a 95% confidence interval (CI) in the participants. The ICC value is considered to be acceptable when it falls between 0.75 and 0.90 and is excellent when >0.90 [29].

Statistical analysis

Statistical analyses were performed using the Statistical Package for the Social Sciences (SPSS) software (SPSS Inc., version 22; Chicago, IL, USA). The normality of data was tested using both visual (histograms and probability plots) and analytical (Kolmogorov–Smirnov/Shapiro–Wilk test) methods. The descriptive analysis was expressed as a mean value along with the standard deviation. While a paired samples *t*-test was employed to test the significance of pairwise differences between both eyes of patients with clinically unilateral XFS, an independent samples *t*-test was used to assess the significance between the right eye of control participants and each eye of patients with XFS. A Bonferroni correction was applied for multiple pairwise comparisons. The Levene test was employed to check the homogeneity of the variances. The Chi-square test was used to analyse the categorical variables. A p value < 0.05 was considered statistically significant.

Results

In this study, 100 eyes of 50 clinically unilateral XFS cases (50 affected eyes and 50 unaffected fellow eyes) and 50 eyes of 50 healthy participants were included. There was no significant difference between the patient and control groups with respect to age (58.3 ± 3.5 vs. 57.6 ± 3.3, respectively; $p = 0.411$) and distribution of gender (28 females vs. 30 females, respectively; $p = 0.302$). There were no significant differences among the groups in terms of the BCVA, SE, IOP, CCT, AL, MAP, and MOPP ($p > 0.05$ for all comparisons). We also found no significant differences in the RNFL thickness analysis by OCT among the groups ($p > 0.05$ for all comparisons, Table 1).

Table 2 shows the choroidal vascular measurements of the submacular and peripapillary regions among the groups. The mean mCVI values of the affected eyes were significantly lower compared to the control eyes on both horizontal and vertical macular scans (60.08 ± 2.06 vs. 67.31 ± 2.24; $p = 0.001$ and 62.21 ± 2.10 vs. 68.11 ± 2.36; $p < 0.001$, respectively). Furthermore, the mean LSR values of the affected eyes were significantly lower compared with the control eyes on both the horizontal and vertical macular scans (1.556 ± 0.162 vs. 2.059 ± 0.195; $p < 0.001$ and 1.646 ± 0.165 vs. 2.136 ± 0.206; $p < 0.001$, respectively). There were no significant differences between the unaffected fellow and control eyes in terms of the mCVI and

Table 1 Demographic and clinical characteristics of the participants.

	Affected eyes ($n = 50$)	Unaffected fellow eyes ($n = 50$)	Control eyes ($n = 50$)	P value
Age (years)	58.3 ± 3.5	58.3 ± 3.5	57.6 ± 3.3	0.411[a]
Sex (m/f)	22/28	22/28	20/30	0.302[b]
BCVA (LogMAR)	0.04 ± 0.02	0.03 ± 0.01	0.02 ± 0.01	0.162[c], 0.354[d], 0.386[e]
SE (D)	− 1.03 ± 0.08	−1.10 ± 0.11	−0.95 ± 0.07	0.461[c], 0.330[d], 0.602[e]
IOP (mmHg)	16.3 ± 2.2	15.9 ± 2.0	16.4 ± 2.2	0.807[c], 0.245[d], 0.321[e]
CCT (μm)	532.5 ± 26.9	536.2 ± 29.0	535.6 ± 27.4	0.224[c], 0.773[d], 0.190[e]
AL (mm)	23.27 ± 0.33	23.35 ± 0.38	23.41 ± 0.36	0.113[c], 0.327[d], 0.286[e]
RNFL thickness (μm)				
Mean	97.9 ± 9.4	98.3 ± 9.1	99.4 ± 9.2	0.307[c], 0.555[d], 0.826[e]
Superior	119.8 ± 17.2	120.6 ± 17.5	122.7 ± 16.8	0.188[c], 0.301[d], 0.665[e]
Inferior	124.1 ± 18.2	124.3 ± 17.8	126.2 ± 17.1	0.444[c], 0.517[d], 0.851[e]
Temporal	70.1 ± 12.3	70.6 ± 12.6	70.4 ± 12.6	0.546[c], 0.678[d], 0.492[e]
Nasal	77.7 ± 14.5	77.8 ± 14.7	78.5 ± 15.0	0.422[c], 0.451[d], 0.873[e]
MAP (mmHg)	97.2 ± 8.0	97.2 ± 8.0	95.9 ± 7.1	0.229[a]
MOPP (mmHg)	48.5 ± 4.7	48.9 ± 4.7	47.5 ± 4.4	0.217[c], 0.175[d], 0.420[e]

BCVA best-corrected visual acuity, *D* diopter, *SE* spherical equivalent, *IOP* intraocular pressure, *CCT* central corneal thickness, *AL* axial length, *RNFL* retinal nerve fiber layer, *MAP* mean arterial pressure, *MOPP* mean ocular perfusion pressure.

[a]Comparison between patients with XFS and control group (Independent samples *t*-test).

[b]Comparison between patients with XFS and control group (Chi-square test).

[c,d,e]Pairwise comparisons with Bonferroni correction ([c]Independent samples *t*-test between affected and control eyes, [d]Independent samples *t*-test between unaffected fellow and control eyes, [e]Paired samples *t*-test between affected and unaffected fellow eyes).

LSR in horizontal and vertical scans of the submacular region ($p > 0.05$ for all).

The mean pCVI values of the temporal, superior, and inferior sectors were significantly lower in affected eyes compared to control eyes (58.73 ± 3.15 vs. 63.21 ± 3.07; $p < 0.001$, 59.84 ± 3.09 vs. 62.07 ± 3.05; $p = 0.002$, 56.94 ± 2.47 vs. 60.78 ± 2.88; $p < 0.001$, respectively). The mean LSR values of the temporal, superior, and inferior peripapillary sectors were significantly lower in the affected eyes compared with the control eyes (1.423 ± 0.187 vs. 1.718 ± 0.165; $p = 0.001$, 1.490 ± 0.205 vs. 1.636 ± 0.198; $p = 0.005$, 1.322 ± 0.165 vs. 1.551 ± 0.171; $p = 0.003$, respectively). The unaffected fellow eyes had significantly lower pCVI values in the temporal and inferior sectors compared to the control eyes (61.42 ± 3.07 vs. 63.21 ± 3.00; $p = 0.007$ and 57.61 ± 2.56 vs. 60.78 ± 2.88; $p = 0.005$, respectively). In addition, the unaffected fellow eyes had lower LSR values in the temporal and inferior sectors compared with the control eyes (1.592 ± 0.194 vs. 1.718 ± 0.165; $p = 0.002$ and 1.359 ± 0.152 vs. 1.551 ± 0.171; $p = 0.006$, respectively). There were no significant differences in the pCVI and LSR values of the nasal peripapillary sector among the groups ($p > 0.05$ for all comparisons, Table 2).

The intraclass correlation coefficient for our study showed excellent interobserver and intraobserver reliability agreement with a range from 0.919–0.951 (0.888–0.963 with 95% CI) for the former and 0.974–0.994 (0.959–0.997 with 95% CI) for the latter (Table 3).

Discussion

Vascular dysfunction is frequently associated with XFS. Pseudoexfoliation material accumulates in vascular endothelial cells, smooth muscle cells, and pericytes and causes microcirculation impairment [5, 30, 31]. XFS, especially the type that involves small vessels and causes ischemic changes in organs, has also been found to be associated with cerebrovascular and cardiovascular dysfunction [32]. XFS is also an important risk factor for glaucoma development. The presence of XFS in cases with ocular hypertension had a two to three times higher risk than patients with ocular hypertension without XFS [33, 34]. Increased IOP caused by aqueous humour outflow resistance due to the deposition of XFM, structural and functional alterations to and increased vulnerability of the lamina cribrosa, and anterior displacement of the crystalline lens due to zonular weakness are the main factors involved in the development of pseudoexfoliative glaucoma [35]. Furthermore, vascular dysfunction plays an important role in the pathogenesis of glaucoma [36]. It is thought that a low ocular perfusion pressure leads to ischemic damage and glaucomatous changes in the optic nerve head [37].

Table 2 Choroidal vascular measurements of the submacular and peripapillary regions.

	Affected eyes ($n = 50$)	Unaffected fellow eyes ($n = 50$)	Control eyes ($n = 50$)	P value[a] (Affected vs. control)	P value[a] (Unaffected fellow vs. control)	P value[b] (Affected vs. unaffected fellow)
Macula						
Mean						
TCA (mm^2)	0.741 ± 0.099	0.746 ± 0.104	0.775 ± 0.090	0.118	0.137	0.715
LA (mm^2)	0.456 ± 0.040	0.497 ± 0.051	0.524 ± 0.042	**0.001**	0.142	**0.007**
SA (mm^2)	0.285 ± 0.028	0.249 ± 0.031	0.250 ± 0.026	0.057	0.847	0.094
LSR	1.601 ± 0.163	1.995 ± 0.208	2.099 ± 0.200	**<0.001**	0.103	**0.001**
CVI (%)	61.49 ± 2.08	66.62 ± 2.45	67.61 ± 2.30	**0.001**	0.106	**0.001**
Horizontal						
TCA (mm^2)	0.750 ± 0.103	0.734 ± 0.100	0.768 ± 0.094	0.186	0.111	0.368
LA (mm^2)	0.456 ± 0.042	0.482 ± 0.047	0.517 ± 0.039	**0.005**	0.106	**0.008**
SA (mm^2)	0.293 ± 0.031	0.252 ± 0.029	0.251 ± 0.024	**0.011**	0.870	0.070
LSR	1.556 ± 0.162	1.920 ± 0.202	2.059 ± 0.195	**<0.001**	0.055	**0.001**
CVI (%)	60.08 ± 2.06	65.66 ± 2.40	67.31 ± 2.24	**0.001**	0.094	**0.002**
Vertical						
TCA (mm^2)	0.733 ± 0.096	0.757 ± 0.107	0.781 ± 0.085	0.091	0.221	0.116
LA (mm^2)	0.456 ± 0.039	0.511 ± 0.053	0.532 ± 0.044	**<0.001**	0.208	**0.006**
SA (mm^2)	0.277 ± 0.025	0.246 ± 0.033	0.249 ± 0.027	0.068	0.606	0.082
LSR	1.646 ± 0.165	2.077 ± 0.213	2.136 ± 0.206	**<0.001**	0.145	**<0.001**
CVI (%)	62.21 ± 2.10	67.50 ± 2.49	68.11 ± 2.36	**<0.001**	0.120	**0.001**
Peripapillary						
Mean						
TCA (mm^2)	0.210 ± 0.027	0.205 ± 0.025	0.206 ± 0.024	0.335	0.712	0.307
LA (mm^2)	0.125 ± 0.022	0.125 ± 0.021	0.127 ± 0.018	0.682	0.677	0.898
SA (mm^2)	0.084 ± 0.009	0.080 ± 0.008	0.078 ± 0.007	0.097	0.440	0.213
LSR	1.488 ± 0.174	1.562 ± 0.181	1.628 ± 0.172	**0.008**	**0.016**	**0.038**
CVI (%)	59.52 ± 2.85	60.97 ± 2.92	62.03 ± 2.81	**0.001**	**0.011**	**0.020**
Temporal						
TCA (mm^2)	0.206 ± 0.032	0.197 ± 0.028	0.193 ± 0.024	0.126	0.434	0.201
LA (mm^2)	0.121 ± 0.024	0.121 ± 0.021	0.122 ± 0.017	0.567	0.502	0.555
SA (mm^2)	0.085 ± 0.011	0.076 ± 0.010	0.071 ± 0.008	**0.013**	0.060	**0.015**
LSR	1.423 ± 0.187	1.592 ± 0.194	1.718 ± 0.165	**0.001**	**0.002**	**0.004**
CVI (%)	58.73 ± 3.15	61.42 ± 3.07	63.21 ± 3.00	**<0.001**	**0.007**	**0.002**
Superior						
TCA (mm^2)	0.254 ± 0.046	0.252 ± 0.041	0.261 ± 0.041	0.180	0.113	0.446
LA (mm^2)	0.152 ± 0.033	0.155 ± 0.032	0.162 ± 0.023	0.097	0.159	0.211
SA (mm^2)	0.102 ± 0.008	0.097 ± 0.008	0.099 ± 0.008	0.419	0.562	0.333
LSR	1.490 ± 0.205	1.598 ± 0.216	1.636 ± 0.198	**0.005**	0.115	**0.010**
CVI (%)	59.84 ± 3.09	61.51 ± 3.15	62.07 ± 3.05	**0.002**	0.103	**0.009**
Nasal						
TCA (mm^2)	0.235 ± 0.026	0.222 ± 0.024	0.215 ± 0.027	0.215	0.317	0.286
LA (mm^2)	0.145 ± 0.017	0.138 ± 0.017	0.133 ± 0.020	0.109	0.213	0.212
SA (mm^2)	0.090 ± 0.009	0.084 ± 0.008	0.082 ± 0.007	0.056	0.509	0.130
LSR	1.611 ± 0.155	1.642 ± 0.173	1.621 ± 0.161	0.221	0.106	0.085
CVI (%)	61.70 ± 2.51	62.16 ± 2.87	61.86 ± 2.46	0.170	0.098	0.087
Inferior						
TCA (mm^2)	0.144 ± 0.010	0.151 ± 0.021	0.153 ± 0.019	0.056	0.404	0.088
LA (mm^2)	0.082 ± 0.007	0.087 ± 0.011	0.093 ± 0.012	0.098	0.183	0.141
SA (mm^2)	0.062 ± 0.006	0.064 ± 0.007	0.060 ± 0.005	0.590	0.257	0.386
LSR	1.322 ± 0.165	1.359 ± 0.152	1.551 ± 0.171	**0.003**	**0.006**	0.143
CVI (%)	56.94 ± 2.47	57.61 ± 2.56	60.78 ± 2.88	**<0.001**	**0.005**	0.098

Bold values indicate statistical significance.

CVI choroidal vascularity index, *LA* luminal area, *LSR* luminal-to-stromal ratio, *SA* stromal area, *TCA* total choroidal area.

[a,b]Pairwise comparisons with Bonferroni correction ([a]Independent samples *t*-test, [b]Paired samples *t*-test).

Table 3 Intraclass correlation coefficient for CVI measurement in the participants.

	Interobserver variability (95% CI)	Intraobserver variability (95% CI)
Macula		
Horizontal	0.945 (0.921–0.958)	0.982 (0.969–0.991)
Vertical	0.951 (0.925–0.962)	0.988 (0.976–0.994)
Peripapillary		
Temporal	0.919 (0.888–0.934)	0.974 (0.959–0.985)
Superior	0.950 (0.923–0.963)	0.986 (0.976–0.991)
Nasal	0.938 (0.903–0.956)	0.988 (0.978–0.992)
Inferior	0.940 (0.910–0.957)	0.994 (0.980–0.997)

CVI choroidal vascularity index, *CI* confidence interval.

The CVI is a novel marker that provides information about the choroidal vascular architecture using a binarization method [38]. In this study, we evaluated the submacular and peripapillary choroidal vascular network in the affected and unaffected eyes of patients with clinically unilateral XFS and compared the findings with those from healthy eyes. To the best of our knowledge, this is the first study to investigate choroidal vascular status using an image binarization technique in unilateral XFS. Our results showed a statistically significant decrease in the pCVI and mCVI values in the affected eyes of clinically unilateral XFS cases compared to control eyes. These results may be important to determine the vascular and/or ischemic pathway in the progression to glaucoma in these patients. Furthermore, the pCVI values of the temporal and inferior sectors were lower in the unaffected fellow eyes of patients with clinically unilateral XFS than in the control eyes. This difference may indicate that although XFM is not clinically observed in unaffected fellow eyes, it may still cause microstructural changes. However, no significant difference in the mCVI was found between the unaffected fellow and control eyes.

Quantitative parameters for the choroid in ocular diseases have been extensively studied and have attracted much attention. The most known of these markers is the CT measurement. In previous studies, various results related to CT have been reported in XFS. Eroglu et al. [39] found thinner choroids in the affected eyes of patients with unilateral XFS than in their unaffected fellow eyes and in the healthy eyes (237.35 ± 58.01, 330.75 ± 47.84, 311.8 ± 51.42 µm, respectively). Similarly, Turan-Vural et al. [16] detected decreased CT in eyes with XFS compared to control eyes (249.4 ± 46.3 vs. 282.5 ± 55.8 µm, respectively). In addition to these aforementioned studies, Dursun et al. [40] identified thinning not only in the subfoveal region (223.96 ± 81.51 vs. 280.10 ± 63.83 µm, respectively) but also in the peripapillary region (131.33 ± 46.82 vs. 156.59 ± 33.84 µm, respectively) when compared with control participants. In contrast, Zengin et al. [19] reported no difference in CT between XFS and control cases (206.6 ± 37.6 vs. 215.9 ± 47.3 µm, respectively). Ozge et al. [20] identified no difference between XFS and healthy eyes in both subfoveal CT (295.0 ± 80.0 vs. 263.0 ± 101.9 µm, respectively) and peripapillary CT (155.8 [75.5–313.1] vs. 155.0 [76–283] µm, respectively).

These conflicting results in the literature may be due to the clinician's experience, the variety of imaging tools used, and the ethnicity differences of the included patients. In addition, the lack of a certain rationality of the distance from the fovea (500, 1000, or 2000 µm) in the CT measurements may have influenced the results. Since the choroid is composed of blood vessels and connective tissue, CT is a measurement that indirectly reveals the vascular structure [15]. The CVI was first described by Agrawal et al. and only allows for an evaluation of the vascular area in the choroid [22, 38]. While CT assesses local measurement points at a certain distance from the fovea, the CVI may provide more precise information about the percentage of the LA in the entire selected area in the choroid. When compared to CT, the CVI appears to be a more robust marker for evaluating the vascular status of the choroid, as it is not associated with most physiological variables, such as age, axial length, refractive error, IOP, SBP, and diurnal variation [15].

The CVD, which is obtained by OCT, is another quantitative marker related to the choroid [41, 42]. This value is achieved by measuring the diameters of the hyporeflective areas in the choroid. Sarrafpour et al. showed that choroidal vessel diameters are smaller in the affected eyes of patients with unilateral XFS when compared to their contralateral unaffected eyes [18]. However, the CVD is insufficient to give information about the total choroidal area. Normal healthy patients may have various choroidal variations [15]. Therefore, rather than evaluating the choroid vessels separately, examining the entire choroid provides valuable information.

Other methods of choroidal vascularity analysis have been studied. Ocular blood flow changes illustrating the nature of vascular impairment were explored in XFS patients. Yüksel et al. detected reduced hemodynamic parameters in the retrobulbar vessels [12]; Dayanır et al. showed reduced ophthalmic artery hemodynamic parameters with colour Doppler imaging in XFS [13]. As a result of these studies, it was concluded that XFS caused a decrease in blood flow velocities and an increase in vascular resistance.

Our study had some limitations. The first was the small number of patients who met the inclusion criteria. Second, the cross-sectional method used in our study was unable to provide information about the progression of these patients. Cohort studies will be needed to analyse the vascular

pathway more meaningfully in glaucoma pathogenesis. However, our study included preliminary findings regarding pseudoexfoliation in the CVI and will be of value to future studies. Third, there were some technical limitations that could result in CVI variations, such as a lack of spatial resolution to distinguish the luminal and stromal components of the choriocapillaris with current technology, shadowing of larger retinal vascular structures on the choroid, or poor-quality images in general [15]. However, in our study, only high-quality images were included to minimize variations in the CVI. In addition, the high ICC value is another strength of our study.

In conclusion, eyes with XFS showed a significant decrease in both the peripapillary CVI and submacular CVI values compared to control eyes. Our results suggest that XFM may be associated with choroidal vascular involvement. In addition, peripapillary choroidal vascularity in the unaffected eyes of unilateral XFS patients were significantly different than the characteristics of healthy control participants. This observation may indicate the presence of subclinical effects of XFM in unaffected fellow eyes. These findings are remarkably important in terms of identifying the vascular pathway of these cases in the development of glaucoma. An extensive series of studies and further analyses will be needed to determine the effects of exfoliation on the vascular structure and its role in glaucoma development.

Summary

What was known before

- Pseudoexfoliation syndrome is a systemic disease with vascular involvement. This condition causes changes in measurements of the choroidal thickness and choroidal vessel diameter.

What this study adds

- The affected eyes of cases with clinically unilateral pseudoexfoliation syndrome shows a decrease in the peripapillary and macular choroidal vascularity index. Furthermore, the unaffected fellow eyes have a decrease in the peripapillary choroidal vascularity. These findings indicate the presence of choroidal vascular involvement in pseudoexfoliation syndrome. Furthermore, our results support the bilateral asymmetric nature of this condition.

Funding The authors indicate they have no financial disclosures. The authors, their families, their employers and their business associates have no financial or proprietary interest in any product or company associated with any device, instrument or drug mentioned in this article. The authors have not received any payment as consultants, reviewers or evaluators of any of the devices, instruments or drugs mentioned in this article.

Compliance with ethical standards

Conflict of interest The authors declare that they have no conflict of interest.

Ethical approval All procedures performed in studies involving human participants were in accordance with the ethical standards of the Ankara Education and Research Hospital (Report Number: 2019-113) and with the 1964 Helsinki Declaration and its later amendments or comparable ethical standards.

References

1. Plateroti P, Plateroti AM, Abdolrahimzadeh S, Scuderi G. Pseudoexfoliation syndrome and pseudoexfoliation glaucoma: a review of the literature with updates on surgical management. J Ophthalmol. 2015;2015:370371.
2. Ritch R. Ocular findings in exfoliation syndrome. J Glaucoma 2018;27:S67–71.
3. Elhawy E, Kamthan G, Dong CQ, Danias J. Pseudoexfoliation syndrome, a systemic disorder with ocular manifestations. Hum Genom. 2012;6:22.
4. Schlötzer-Schrehardt U, Naumann GO. Ocular and systemic pseudoexfoliation syndrome. Am J Ophthalmol. 2006;141:921–37.
5. Praveen MR, Shah SK, Vasavada AR, Diwan RP, Shah SM, Zumkhawala BR, et al. Pseudoexfoliation as a risk factor for peripheral vascular disease: a case-control study. Eye. 2011;25:174–9.
6. Gonen KA, Gonen T, Gumus B. Renal artery stenosis and abdominal aorta aneurysm in patients with pseudoexfoliation syndrome. Eye. 2013;27:735–41.
7. Demir N, Ulus T, Yucel OE, Kumral ET, Singar E, Tanboga HI. Assessment of myocardial ischaemia using tissue Doppler imaging in pseudoexfoliation syndrome. Eye. 2011;25:1177–80.
8. Holló G1. Vascular dysfunction in exfoliation syndrome. J Glaucoma. 2018;27:S72–4.
9. Helbig H, Schlötzer-Schrehardt U, Noske W, Kellner U, Foerster MH, Naumann GO. Anterior-chamber hypoxia and iris vasculopathy in pseudoexfoliation syndrome. Ger J Ophthalmol. 1994;3:148–53.
10. Parodi MB, Bondel E, Saviano S, Ravalico G. Iris indocyanine green angiography in pseudoexfoliation syndrome and capsular glaucoma. Acta Ophthalmol Scand. 2000;78:437–42.
11. Schlötzer-Schrehardt U, Küchle M, Naumann GO. Electron-microscopic identification of pseudoexfoliation material in extrabulbar tissue. Arch Ophthalmol. 1991;109:565–70.
12. Yüksel N, Karabaş VL, Arslan A, Demirci A, Cağlar Y. Ocular hemodynamics in pseudoexfoliation syndrome and pseudoexfoliation glaucoma. Ophthalmology. 2001;108:1043–9.
13. Dayanir V, Topaloğlu A, Ozsunar Y, Keceli M, Okyay P, Harris A. Orbital blood flow parameters in unilateral pseudoexfoliation syndrome. Int Ophthalmol. 2009;29:27–32.
14. Cinar E, Yuce B, Aslan F. Retinal and choroidal vascular changes in eyes with pseudoexfoliation syndrome: a comparative study

using optical coherence tomography angiography. Balk Med J. 2019;37:9–14.
15. Agrawal R, Ding J, Sen P, Rousselot A, Chan A, Nivison-Smith L, et al. Exploring choroidal angioarchitecture in health and disease using choroidal vascularity index. Prog Retin Eye Res. 2020; https://doi.org/10.1016/j.preteyeres.2020.100829.
16. Turan-Vural E, Yenerel N, Okutucu M, Yildiz E, Dikmen N. Measurement of subfoveal choroidal thickness in pseudoexfoliation syndrome using enhanced depth imaging optical coherence tomography. Ophthalmologica. 2015;233:204–8.
17. Goktas S, Sakarya Y, Ozcimen M, Sakarya R, Bukus A, Ivacik IS, et al. Choroidal thinning in pseudoexfoliation syndrome detected by enhanced depth imaging optical coherence tomography. Eur J Ophthalmol. 2014;24:879–84.
18. Sarrafpour S, Adhi M, Zhang JY, Duker JS, Krishnan C. Choroidal vessel diameters in pseudoexfoliation and pseudoexfoliation glaucoma analyzed using spectral-domain optical coherence tomography. J Glaucoma. 2017;26:383–9.
19. Zengin MO, Cinar E, Karahan E, Tuncer I, Yilmaz S, Kocaturk T, et al. Choroidal thickness changes in patients with pseudoexfoliation syndrome. Int Ophthalmol. 2015;35:513–7.
20. Ozge G, Koylu MT, Mumcuoglu T, Gundogan FC, Ozgonul C, Ayyildiz O, et al. Evaluation of retinal nerve fiber layer thickness and choroidal thickness in pseudoexfoliative glaucoma and pseudoexfoliative syndrome. Postgrad Med. 2016;128:444–8.
21. You QS, Xu L, Wang YX, Yang H, Ma K, Li JJ, et al. Pseudoexfoliation: normative data and associations: the Beijing eye study 2011. Ophthalmology. 2013;120:1551–8.
22. Agrawal R, Salman M, Tan KA, Karampelas M, Sim DA, Keane PA, et al. Choroidal vascularity index (CVI)–a novel optical coherence tomography parameter for monitoring patients with panuveitis? PLoS One. 2016;11:e0146344.
23. Nickla DL, Wallman J. The multifunctional choroid. Prog Retin Eye Res. 2010;29:144–68.
24. Kim RY, Chung DH, Kim M, Park YH. Use of choroidal vascularity index for choroidal structural evaluation in central serous chorioretinopathy with choroidal neovascularization. Retina. 2019; https://doi.org/10.1097/IAE.0000000000002585.
25. Wei X, Mishra C, Kannan NB, Holder GE, Khandelwal N, Kim R, et al. Choroidal structural analysis and vascularity index in retinal dystrophies. Acta Ophthalmol. 2019;97:e116–21.
26. Pellegrini M, Giannaccare G, Bernabei F, Moscardelli F, Schiavi C, Campos EC. Choroidal vascular changes in arteritic and non-arteritic anterior ischemic optic neuropathy. Am J Ophthalmol. 2019;205:43–9.
27. Cetin EN, Parca O, Akkaya HS, Pekel G. Association of retinal biomarkers and choroidal vascularity index on optical coherence tomography using binarization method in retinitis pigmentosa. Graefes Arch Clin Exp Ophthalmol. 2020;258:23–30.
28. Wang W, Zhou M, Huang W, Chen S, Ding X, Zhang X. Does acute primary angle-closure cause an increased choroidal thickness? Investig Ophthalmol Vis Sci. 2013;54:3538–45.
29. Koo TK, Li MY. A guideline of selecting and reporting intraclass correlation coefficients for reliability research. J Chiropr Med. 2016;15:155–63.
30. Atalar PT, Atalar E, Kilic H, Abbasoglu OE, Ozer N, Aksöyek S, et al. Impaired systemic endothelial function in patients with pseudoexfoliation syndrome. Int Heart J. 2006;47:77–84.
31. Wang W, He M, Zhou M, Zhang X. Ocular pseudoexfoliation syndrome and vascular disease: a systematic review and meta-analysis. PLoS One. 2014;9:e92767.
32. Chung H, Arora S, Damji KF, Weis E. Association of pseudoexfoliation syndrome with cardiovascular and cerebrovascular disease: a systematic review and meta-analysis. Can J Ophthalmol. 2018;53:365–72.
33. Grødum K, Heijl A, Bengtsson B. Risk of glaucoma in ocular hypertension with and without pseudoexfoliation. Ophthalmology. 2005;112:386–90.
34. Leske MC, Heijl A, Hyman L, Bengtsson B, Dong L, Yang Z, et al. Predictors of long-term progression in the early manifest glaucoma trial. Ophthalmology. 2007;114:1965–72.
35. Ozaki M. Mechanisms of glaucoma in exfoliation syndrome. J Glaucoma. 2018;27:S83–6.
36. Grieshaber MC, Mozaffarieh M, Flammer J. What is the link between vascular dysregulation and glaucoma? Surv Ophthalmol. 2007;52:S144–54.
37. Flammer J, Orgül S, Costa VP, Orzalesi N, Krieglstein GK, Serra LM, et al. The impact of ocular blood flow in glaucoma. Prog Retin Eye Res. 2002;21:359–93.
38. Agrawal R, Gupta P, Tan KA, Cheung CM, Wong TY, Cheng CY. Choroidal vascularity index as a measure of vascular status of the choroid: Measurements in healthy eyes from a population-based study. Sci Rep. 2016;6:21090.
39. Eroglu FC, Asena L, Simsek C, Kal A, Yılmaz G. Evaluation of choroidal thickness using enhanced depth imaging by spectral-domain optical coherence tomography in patients with pseudoexfoliation syndrome. Eye. 2015;29:791–6.
40. Dursun A, Ozec AV, Dogan O, Dursun FG, Toker MI, Topalkara A, et al. Evaluation of choroidal thickness in patients with pseudoexfoliation syndrome and pseudoexfoliation glaucoma. J Ophthalmol. 2016;2016:3545180.
41. Yang L, Jonas JB, Wei W. Choroidal vessel diameter in central serous chorioretinopathy. Acta Ophthalmol. 2013;91:e358–e362.
42. Park KA, Oh SY. An optical coherence tomography-based analysis of choroidal morphologic features and choroidal vascular diameter in children and adults. Am J Ophthalmol. 2014;158:716–23.e2.